Fisheries Research 105 (2010) 91–101

Contents lists available at ScienceDirect

Fisheries Research

journal homepage: www.elsevier.com/locate/fishres

Analysis of longitudinal growth increment data using mixed-effects models: Individual and spatial variability in a clam

Gabriela Escati-Peñaloza*, Ana M. Parma, J.M. (Lobo) Orensanz

Centro Nacional Patagónico (CENPAT/CONICET), Blvd. Brown 2915, 9120 Puerto Madryn, Chubut, Argentina

ARTICLE INFO

Article history:
Received 24 October 2009
Received in revised form 4 March 2010
Accepted 5 March 2010

Keywords:
Ameghinomya
Clam growth
Longitudinal data
Mixed-effects models
Argentina

ABSTRACT

Modeling growth is required in many ecological studies and stock assessment applications, but most fish and shellfish growth analyses focus on the estimation of average parameters, which do not provide a complete description of the growth of members of a population. We investigated individual and spatial variation of growth in striped clams (*Ameghinomya antiqua*) from San Jose Gulf (Argentine Patagonia) using series of growth ring measurements obtained from individual clams from seven populations ("longitudinal data"). Data showed a clear geographical pattern, with two clusters of locations corresponding to domains separated by a thermal front. In the West Domain circulation is dominated by strong tidal-driven eddy flushing, temperature is lower during the growth season, and nutrient concentration and primary productivity are generally higher; circulation is sluggish in the East Domain. West of the front (i) growth rate of small clams and maximum growth rate are highest, and (ii) individual growth rate tends to peak at a smaller size and at a younger age. Evidence of an inflection point in growth rate prompted use of the Richards model, which has been frequently applied to benthic invertebrates for that reason. The model, however, had structural limitations and failed to fit the sharp inflection point. Differences in average parameter values, on the other hand, captured the variability between populations. While all individuals followed the same general growth pattern, there was high variability in individual growth profiles. Accounting for this variability through random effects in all growth parameters affected the estimated average parameters: predicted growth increments at size were larger initially, and the trend reversed after a certain size. Within-individual autocorrelation was not significant, a benefit of using growth increments instead of size-at-age data. We discuss between populations variation in relation to mesoscale environmental gradients, the use of mixed-effects models to analyze longitudinal data, and the implications of our results for stock assessment and management.

© 2010 Elsevier B.V. All rights reserved.

1. Introduction

Modeling growth is required in many ecological studies and stock assessment applications (Quinn and Deriso, 1999; Sebens, 1987), but most fish and shellfish growth analyses focus on the estimation of average parameters, which do not provide a complete description of the growth of members of a population. An adequate representation of growth variability is often just as important as a model for average growth. It is essential in size-structured demographic models (e.g. Punt et al., 2009), and it allows improved representation of size-dependent processes, such as mortality and fecundity, in age-structured models (e.g. Heino et al., 2002; Parma and Deriso, 1990). In addition, individual variability needs to be considered to avoid biases in estimated mean parameters (Eveson et al., 2007; Sainsbury, 1980; Wang and Thomas, 1995).

Variation among individuals can be captured by treating some of the growth parameters as random variables, through either deterministic (e.g. Sainsbury, 1980) or stochastic (e.g. Parma and Deriso, 1990) approaches. In the first case all variability is attributed to intrinsic differences among individuals, whether genetic or phenotypic; in the second there is additional variability affecting each individual growth trajectory. Growth parameters are typically estimated from size-at-age data, where individuals are measured and aged at the time of capture, or alternatively from mark-recapture experiments (Sainsbury, 1980). These kinds of data may be uninformative about underlying sources of growth variability (Eveson et al., 2007), and about how much of it is due to intrinsic or environmental factors. In some situations animals can be measured repeatedly over time, each yielding a series of data points ("longitudinal data", Diggle et al., 2002; Zeger and Liang, 1986). This is the case of repeated observations made on experimental animals or sequences of measures of growth marks on hard-body structures

---

* Corresponding author. Tel.: +54 2965 451024; fax: +54 2965 451543.
E-mail addresses: gescati@cenpat.edu.ar (G. Escati-Peñaloza), parma@cenpat.edu.ar (A.M. Parma), lobo@cenpat.edu.ar (J.M. Orensanz).

0165-7836/$ – see front matter © 2010 Elsevier B.V. All rights reserved.
doi:10.1016/j.fishres.2010.03.007

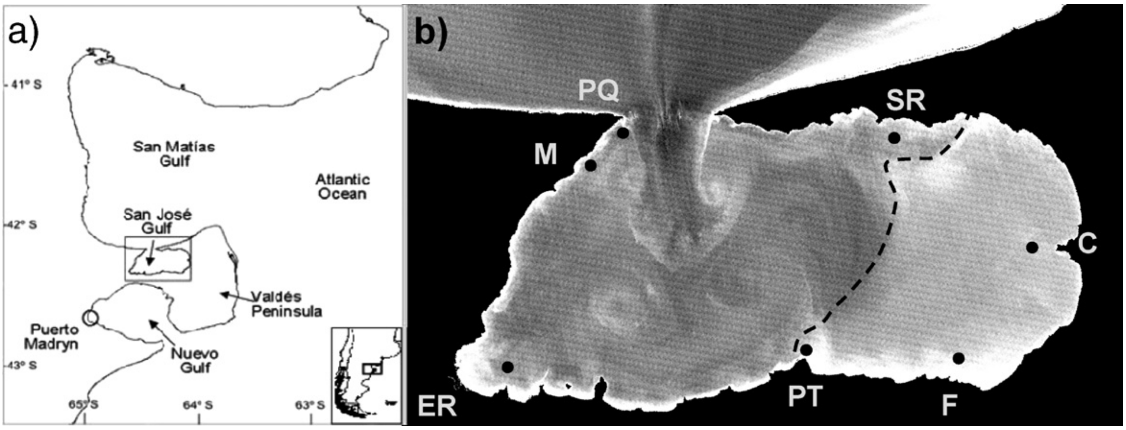

Fig. 1. Study area. (a) The North Patagonian Gulfs. (b) Landsat image of San Jose Gulf showing the spatial distribution of sea surface temperature on 12/05/1998. The dashed line shows the approximate position of the thermal front that divides the gulf in two domains. Study sites: Punta Quiroga (PQ), Mendioroz (M), El Riacho (ER), Punta Tehuelche (PT), Fracaso (F), Conos (C) and San Roman (SR).

(otoliths, scales, shells) (Pilling et al., 2002). A major advantage of longitudinal data is that they allow separation of changes over time within-individuals from differences among individuals relative to a baseline level (Diggle et al., 2002; Fitzmaurice et al., 2004; Hedeker and Gibbons, 2006).

Growth variability in natural populations results from differences in genetic makeup or from environmental effects. Many benthic organisms (e.g. clams) are sedentary and inhabit spatially heterogeneous environments, thus individual growth may vary even over relative small distances (Cerrato and Keith, 1992; Peterson and Beal, 1989; Richardson, 2001). As individual growth profiles are recoverable from hard structures, longitudinal data can be used to investigate spatial patterns in growth incorporating the complete growth history of individuals exposed to different environments (Diggle et al., 2002; Smith et al., 2001; Ware, 1985). Repeated measurements tend to be auto-correlated not only due to intrinsic differences among individuals, but also because environmental factors that affect the growth of sedentary animals are locally persistent or recurrent over time. This must be taken into account when modeling growth; otherwise misleading conclusions could be reached (Diggle et al., 2002; Fitzmaurice et al., 2004; Zeger and Liang, 1986). Mixed-effects models facilitate the incorporation of different sources of growth variability by including *fixed effects*, associated with the population means, which may vary over space, and *random effects*, associated with individual variability (Pinheiro and Bates, 2002). They are increasingly used in the analysis of growth in fisheries applications (Hart and Chute, 2009; Pilling et al., 2002; Schaalje et al., 2002; Smith et al., 2001) due to: (i) their flexibility to model autocorrelation within-individuals, (ii) the possibility of using balanced or unbalanced data, and (iii) the availability of efficient software for parameter estimation (e.g. Lindstrom and Bates, 1990).

In this study we investigated individual and spatial variation of growth in striped clam (*Ameghinomya antiqua* (King, 1831)) populations from San Jose Gulf (Argentine Patagonia) using series of size-at-age measurements obtained from individual clams. First we show consistent spatial patterns revealed by the data, and discuss them in relation to environmental gradients. Second, we use nonlinear mixed-effects models in order to formally analyze individual and spatial variation in the observed growth patterns. We evaluate different growth curves for their ability to fit individual series of growth increments, and for the ability of their parameters to capture spatial patterns of variation. Finally we discuss implications of our results for spatially explicit stock assessment and management, attending to pragmatic considerations.

2. Study system

2.1. Study area

San Jose Gulf (Fig. 1a) is located in Argentine Patagonia, north of Valdes Peninsula, at the transition between the cold-temperate (Magellanic Biogeographic Province) and warm-temperate (Argentine Province) regions of the southwest Atlantic. The gulf has a small elliptical outline, a surface of 814 km^2, an average depth of 38 m, and is connected to the adjacent San Matias Gulf through a narrow entrance. This is a region with low levels of precipitation (180 mm mean annual average), no permanent water courses flowing into the gulf and no significant human settlements along its coasts. The tidal regime is semidiurnal, with average amplitude varying between 6.4 and 1.83 m. A thermal and turbidity front separates two domains with different hydrodynamic and thermal conditions (Fig. 1b): the West Domain, which is highly turbulent due to the development of vortexes and dipoles during the tidal cycle, and the East Domain, which has more sluggish circulation and larger contrast in temperature between summer and winter (Amoroso and Gagliardini, 2010). Nutrient availability is higher in the West Domain throughout the year, while primary productivity is higher only during the summer (Amoroso and Gagliardini, 2010). We selected seven study sites around the perimeter of the gulf, representative of differing oceanographic conditions (Amoroso and Gagliardini, 2010; Charpy and Charpy-Roubaud, 1980; Ciocco, 1991; Esteves et al., 1986). The two sites located to the east of the frontal system (Conos and Fracaso) are characterized by low flushing, long water residence time and relatively low nutrient load throughout the year, and low chlorophyll *a* concentration during summer. The four sites located in the well-mixed West Domain (Punta Quiroga, Mendioroz, El Riacho and San Roman) vary in their productivity and degree of exposure to tidal flushing and associated eddies, El Riacho being the most sheltered and productive, and Punta Quiroga the least. Finally, a site at the southern end of the frontal system (Punta Tehuelche) is directly exposed to eddy flushing and characterized by low productivity and nutrient concentration.

2.2. The striped clam

The striped clam ranges from the intertidal zone to a depth of 100 m. Similar to other cold-temperate species of the Magellanic Biogeographic Province, its geographic range extends northwards to 34°S on the Atlantic and to 12°S on the Pacific (Lasta et al., 1998). Growth rate varies seasonally, rings being associated with

Table 1
Descriptive statistics of striped clam samples collected in the East and West Domains of San Jose Gulf. Domains are separated by a thermal front (see Fig. 1b).

Sampling site	Sampling date	Domain	Shell length (mm)		Growth ring		Maximum growth increment (mm)	Sample size
			Maximum	Inflection point (S.D.)	Maximum	Inflection point (S.D.)		
Punta Quiroga	March 2005	West	77.5	16.11 (8.99)	15	1.9 (0.84)	16.46	25
Mendioroz	April 2003	West	76.2	18.01 (8.06)	11	2.1 (0.77)	15.73	55
El Riacho	April 2003	West	76.8	15.58 (7.08)	13	1.9 (1.41)	17.11	58
Punta Tehuelche	March 2005	East	82.7	23.39 (8.91)	16	2.7 (0.91)	14.64	45
Fracaso 1	August 2004	East	62.2	19.29 (8.09)	10	2.5 (0.94)	15.77	52
Fracaso 2	December 2004	East	73.0	23.84 (10.97)	11	2.5 (1.09)	14.91	41
Conos	August 2004	East	73.9	22.39 (10.94)	14	2.8 (1.20)	13.44	33
San Roman 1	April 2003	West	78.9	17.43 (8.56)	13	1.8 (0.79)	17.64	45
San Roman 2	August 2003	West	73.1	16.54 (8.25)	11	1.9 (0.78)	16.15	54

the winter deceleration of growth (Verdinelli and Schuldt, 1976, and personal observations). The striped clam has an annual reproductive cycle and matures sexually at a size of 20–24 mm, which corresponds to age 1+ in the study region (Verdinelli and Schuldt, 1976). This species supports a significant fishery in Chile (Jerez et al., 1991), and is a potentially important resource for Argentine Patagonia (Lasta et al., 1998). In the San Jose Gulf it is harvested by hookah commercial divers.

3. Material and methods

Samples were collected by hookah divers from clam beds located at the seven study sites described earlier, at depths between 8 and 15 m, the range at which commercial divers usually operate. One sample was collected from each site at Punta Quiroga, Mendioroz, El Riacho, Punta Tehuelche and Conos, and two samples from San Roman and Fracaso; sample size ranged from 25 to 58 individuals (Table 1). Observations were made on the right valve of each clam ($n = 408$); shell length and maximum length of each annual growth ring were measured with calipers (0.1 mm precision). Shells were polished to remove the superficial reticulated sculpture, which obscures growth marks. Maximum size of specimens in the samples ranged from 62.2 to 82.7 mm, and maximum age from 10 to 16 years (Table 1). The work described has been conducted in accordance with The Code of Ethics of the World Medical Association.

4. Theory and estimation

While growth parameters are usually estimated from size-at-age data, we chose instead to use growth increments for three reasons: (1) to reduce the autocorrelation between successive measures taken on the same individual, (2) because the absolute age associated with the first clearly identifiable growth ring is uncertain due to variability in the time at settlement and difficulties in interpreting early growth marks, and (3) the individual profiles of growth increments as a function of shell size are more revealing about growth patterns and sources of variation than are cumulative growth trajectories ("growth curves"). Annual growth increments were calculated as the difference between the maximum lengths of successive growth rings, starting from that between the second and first rings. The size increment between the last growth ring and the shell border was discarded to avoid variability associated with sampling date.

Preliminary inspection of growth increments as a function of shell size indicated the presence of an inflection point. This prompted use of the Chapman–Richards equation (Richards, 1959),

$$L_t = L_\infty\left(1 - \mathrm{e}^{-K(t-t_0)}\right)^{1/(1-M)}, \tag{1}$$

where L_t is length at time t, L_∞ the asymptotic length, K the growth parameter, M the curvature parameter, and t_0 the age at $L_t = 0$. This function has an inflection point at length $L^* = L_\infty M^{1/(1-M)}$ where growth rate is maximum and equal to $dL/dt^* = L_\infty K M^{M/(1-M)}$. The annual size increments, $\Delta L_t = L_{t+1} - L_t$, can be expressed as a function of size:

$$\Delta L_t = L_\infty\left\{1 - \mathrm{e}^{-K}\left[1 - \left(\frac{L_t}{L_\infty}\right)^{1-M}\right]\right\}^{1/(1-M)} - L_t. \tag{2}$$

In addition to the Richards function, the von Bertalanffy model was applied after truncating the data at the second growth ring, the modal ring at which the inflection point occurred. The von Bertalanffy model is a particular case of the Richards model when $M = 0$, implying that there is no inflection point and growth increments are a linear function of size:

$$\Delta L_t = L_\infty(1 - \mathrm{e}^{-K}) - (1 - \mathrm{e}^{-K})L_t. \tag{3}$$

Parameters were estimated using nonlinear mixed-effects models. Growth parameters of each individual clam were expressed as the sum of a population mean parameter ("fixed effect") and an individual deviation ("random effect") (Lindstrom and Bates, 1990). The growth increments of the ith individual, belonging to the p population, were given by

$$\begin{aligned}\Delta L_{t,i} = {} & (L_{\infty,p} + l_{\infty,i}) \\ & \times\left\{1 - \mathrm{e}^{-(K_p+k_i)}\left[1 - \left(\frac{L_{i,t}}{L_{\infty,p} + l_{\infty,i}}\right)^{1-(M_p+m_i)}\right]\right\}^{1/(1-(M_p+m_i))} \\ & - L_{i,t} + \varepsilon_{i,t}\end{aligned} \tag{4}$$

where $L_{\infty,p}$, M_p and K_p represent the average population parameters (fixed effects); $l_{\infty,i}$, m_i and k_i are the random effects, assumed to be normally distributed, with zero mean and variance–covariance matrix $\boldsymbol{D}_i$, a 3×3 matrix with diagonal elements $\sigma^2_{l_\infty}$, σ^2_k and σ^2_m and off-diagonal elements given by $\rho_{l_\infty k}\sigma_{l_\infty}\sigma_k$, $\rho_{l_\infty m}\sigma_{l_\infty}\sigma_m$ and $\rho_{km}\sigma_k\sigma_m$. The term $\varepsilon_{i,t}$ represents process stochasticity assumed to be normally distributed with zero mean and variance–covariance matrix $\sigma^2_\varepsilon \boldsymbol{\Lambda}$. The estimates of $L_{\infty,p}$, M_p and K_p were compared with those obtained from a model that did not incorporate individual variability in growth parameters ($\sigma^2_{l_\infty} = \sigma^2_k = \sigma^2_m = 0$).

The existence of spatial heterogeneity at the scale of the entire study region was evaluated by comparing nested nonlinear models to the full model in which all parameters differed among clam beds. The significance of the differences in mean parameter values (fixed terms) was assessed by conditional F-tests, following Pinheiro and Bates (2002). In the case of random effects, the significance of individual variability in each of the model parameters was evaluated by the likelihood ratio test, under the null hypothesis that the restricted models ($\sigma^2_{l_\infty} = 0$; $\sigma^2_k = 0$ and $\sigma^2_m = 0$) were adequate (Pinheiro and Bates, 2002).

The variance of $\varepsilon_{i,t}$ was assumed to be constant in the Richards model. In the von Bertalanffy model fitted to the truncated data, it was parameterized as a power function of the expected growth increments:

$$\mathrm{Var}(\varepsilon_{i,t}) = \sigma_\varepsilon^2 (E[L_{i,t+1} - L_{i,t}])^{2\delta}.$$

The dependence of sequential observations within-individuals was evaluated by estimating the serial autocorrelation of model residuals using a first-order auto-regressive function.

Growth models were fitted to data from 388 individuals, after excluding individuals with less than four rings, yielding a total of 3328 growth increment observations. Parameters were estimated using maximum likelihood methods implemented in the NLME library (Pinheiro et al., 2007) of the R software (R Development Core Team, 2007, version 2.6.0).

5. Results

5.1. Growth patterns

Annual growth increments increased sharply as a function of shell length at small sizes, reached a maximum at a length between 15 and 20 mm, and decreased thereafter approaching zero at lengths larger than 60 mm (Fig. 2). The inflection point occurred most frequently following the second growth ring (Fig. 3). Thus, if the data are truncated at the second growth ring, growth profiles show a linear decline with shell size. While all individuals fitted this general pattern, there was high variability among populations and among individuals within each population, as evidenced by the spread of the individual growth profiles (Fig. 2).

In order to investigate the existence of spatial gradients in growth we compared the distributions of the individuals' maximum annual growth increment across the nine samples (Fig. 4a). In general, maximum growth rates were lower in populations from the East Domain, and differences in the average maximum growth increments tended to be significant in pair-wise comparisons across domains but not within domains (Fig. 4b). The highest maximum growth rates were observed in El Riacho, San Roman and Mendioroz, all located in the West Domain, and the lowest in Punta Tehuelche and Conos. Punta Tehuelche is located at the pivotal point of the thermal front, exposed directly to eddy flushing. Between these extremes were Fracaso and Punta Quiroga, respectively located at the extremes of a SE–NW axis and exposed to lowest and the highest levels of flushing. Spatial trends in maximum growth rate were negatively correlated with the annual ring at which growth rate is highest; the inflection point occurred later in life (and at larger sizes) in individuals from populations that exhibited relatively low maximum growth rates (Fig. 5, Table 1). Populations fall into two well-defined clusters corresponding to the East and West Domains (Fig. 5).

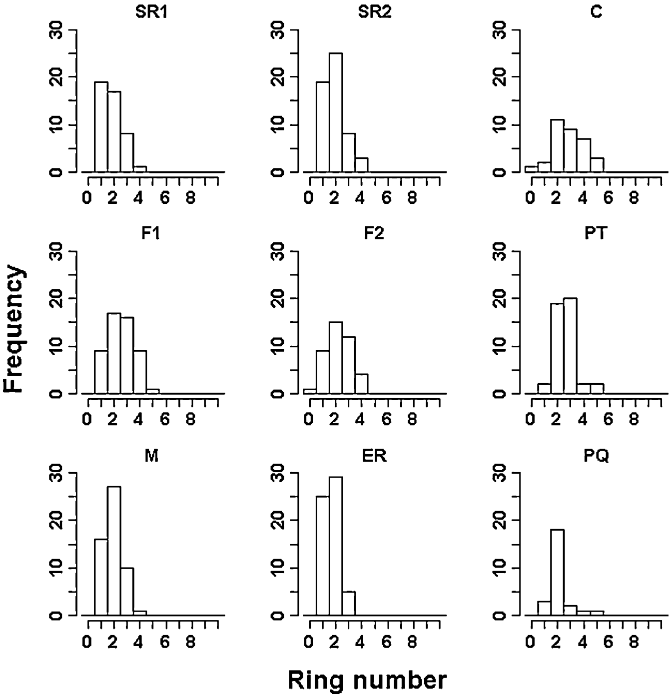

Fig. 3. Frequency distributions of the individual's growth ring number at which growth increment is maximum. Site labels as in Fig. 2.

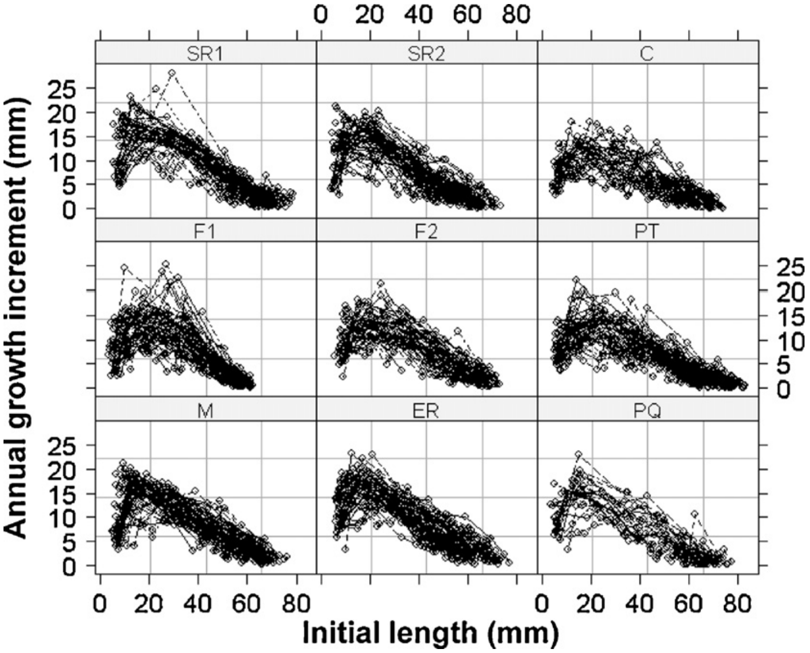

Fig. 2. Individual growth profiles of clams sampled at seven study sites: Punta Quiroga (PQ), Mendioroz (M), El Riacho (ER), Punta Tehuelche (PT), Fracaso (F1 and F2), Conos (C) and San Roman (SR1 and SR2).

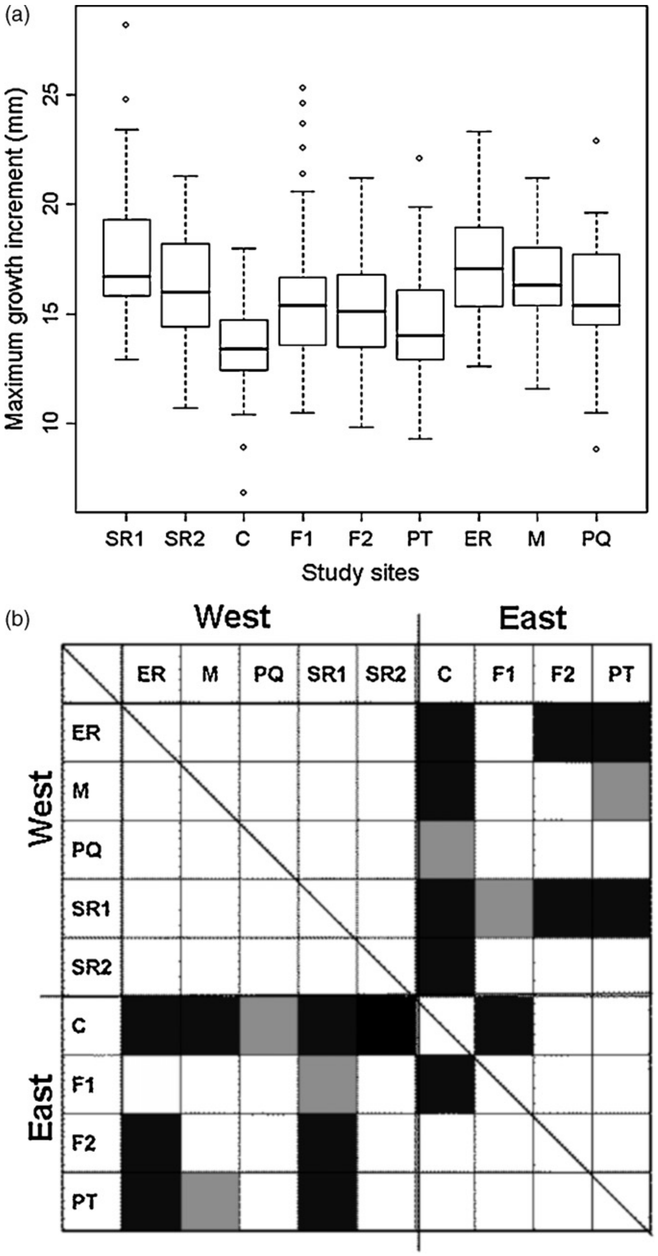

	ER	M	PQ	SR1	SR2	C	F1	F2	PT
ER						■		■	■
M						■			▨
PQ						▨			
SR1						■	▨	■	■
SR2						■			
C	■	■	▨	■	■		■		
F1				▨		■			
F2	■			■					
PT	■	▨		■					

Fig. 4. Between-site comparison of maximum growth increments. (a) Boxplots showing median, first and fourth quartiles and extreme lower and upper whisker; dots indicate outliers. (b) Significance of pair-wise differences between average maximum growth increments based on Tukey's multiple comparison method; black: $^{**}P \leq 0.01$, grey: $^{*}0.01 < P < 0.05$, empty: ns $P \geq 0.05$. Site labels as in Fig. 2.

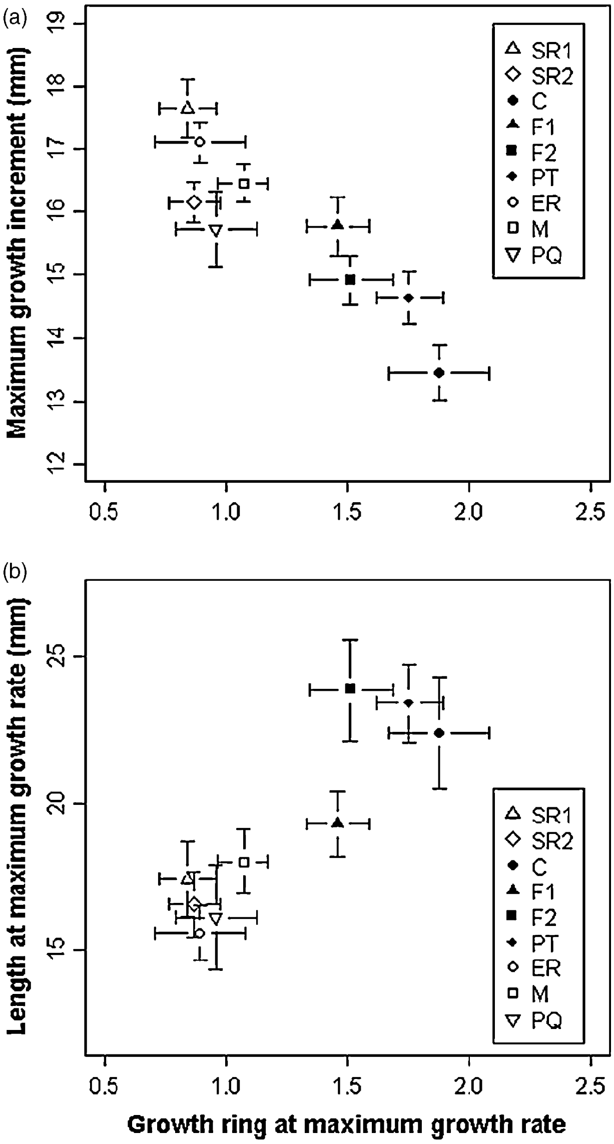

Fig. 5. Relationship between maximum growth increment and growth ring and size at which growth is maximized. Each point corresponds to the average for each study site; bars show ± one standard error. Filled symbols correspond to East Domain, and open symbols to West Domain locations.

5.2. Model selection

When the Richards growth function was fitted to the non-truncated data, incorporation of differences in mean parameter values among populations significantly improved the fits. The comparison of several nested models indicated that there was significant individual variance in addition to the differences in all three fixed parameters (Table 2). The coefficient of variation of the individual growth parameters was close to 7% for L_∞, between 22 and 40% for K, and between 33 and 97% for M; k and m were highly correlated ($\rho_{km} = 0.89$), and l_∞ was negatively correlated with k and m ($\rho_{l_\infty k} = -0.53$ and $\rho_{l_\infty m} = -0.38$).

A comparison of observed and predicted growth increments showed that the Richards model did not adequately represent the growth profiles in any of the populations (Fig. 6). Most individual growth profiles had a sharp inflection point (Fig. 2), which was not captured by the model; this resulted in positive residuals around the inflection point (i.e. at maximum growth rates) and a rather large residual error ($\sigma_\varepsilon = 2.34$).

The von Bertalanffy model provided a good representation of the individual growth profiles above the inflection point (Fig. 7). Again, the model selected was the full model with different fixed parameters among populations and including random effects on both parameters (Table 2). Model residuals increased at larger expected growth increments in all sampled populations (Fig. 8a); the heteroscedasticity was corrected by modeling the variance as a power function of the expected growth increment (Table 2, Fig. 8b). The residuals were serially uncorrelated (estimated autocorrelation equal to 0.0049), which contrasts with the auto-correlated patterns commonly found in analyses of longitudinal data. The coefficient of variation of the individual parameters was between 7 and 8% for L_∞, and between 13 and 17% for K, with a negative correlation coefficient $\rho_{l_\infty k} = -0.60$.

Table 2

Results of model selection using: a) the Richards model and b) the von Bertalanffy model. Differences in mean growth parameters (fixed effects) among populations evaluated with conditional *F*-test. Likelihood ratio test used to assess the significance of individual variability (random effects) and of non-homogeneity of the residual variance (in the von Bertalanffy model). All tests made with respect to the full model. Degrees of freedom of numerator and denominator denoted as df Num and df Den, respectively.

a) Richards model				
	F-test			
Mean parameters	df Num	df Den	*F*-value	*P*
$L_{\infty,p} = L_\infty$	8	2914	41.43	<0.0001
$K_p = K$	8	2914	11.96	<0.0001
$M_p = M$	8	2914	3.04	<0.0001
	Likelihood ratio test			
Variance parameters	df	χ^2-value	*P*	
$\sigma^2_{l_\infty} = 0$	3	116.54	<0.0001	
$\sigma^2_k = 0$	3	52.71	<0.0001	
$\sigma^2_m = 0$	3	79.17	<0.0001	
b) von Bertalanffy model				
	F-test			
Mean parameters	df Num	df Den	*F*-value	*P*
$L_{\infty,p} = L_\infty$	8	379	59.54	<0.0001
$K_p = K$	8	2564	17.61	<0.0001
	Likelihood ratio test			
Variance parameters	df	χ^2-value	*P*	
$\sigma^2_{l_\infty} = 0$	2	52.75	<0.0001	
$\sigma^2_k = 0$	2	125.59	<0.0001	
$\delta = 0$	1	1459.58	<0.0001	

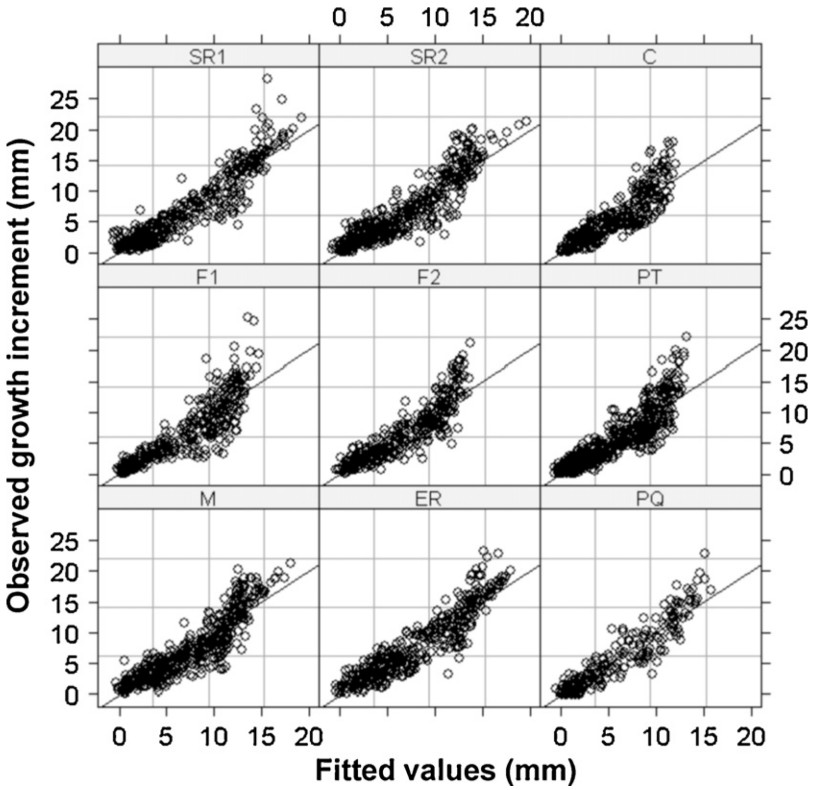

Fig. 6. Scatter plots of observed shell length increments versus fitted values for the mixed-effects version of the Richards model including variability among populations. Site labels as in Fig. 2.

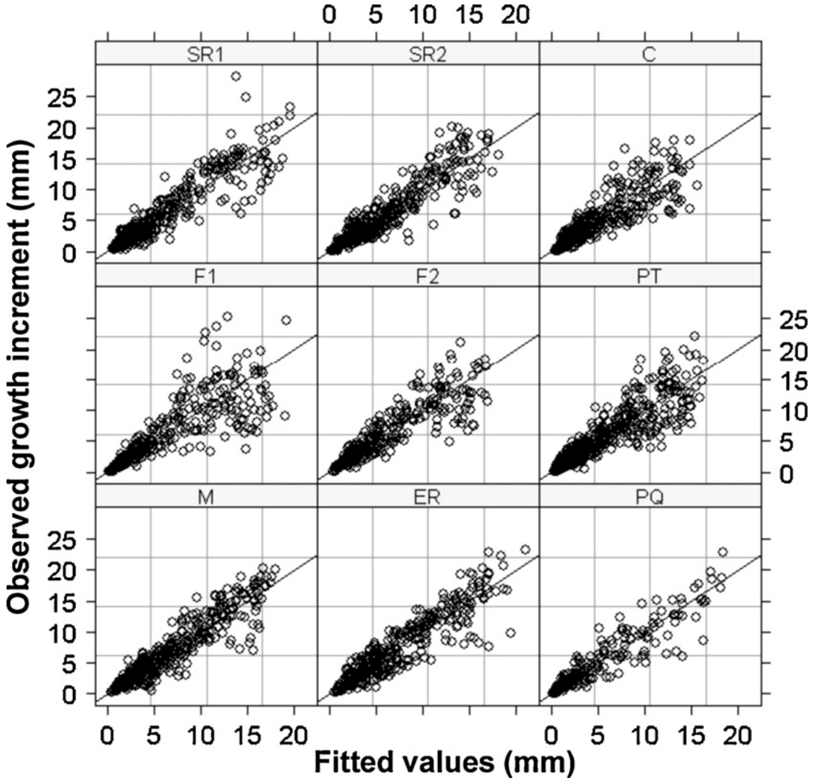

Fig. 7. Scatter plots of observed shell length increments versus fitted values for the mixed-effects version of the von Bertalanffy model including variability among populations. Variance was parameterized as a power function of the expected growth increment. Site labels as in Fig. 2.

Mean population parameters estimated with mixed-effects models differed from those obtained with fixed-effects models that did not include individual variability. This was true for both the Richards (non-truncated data) and the von Bertalanffy (truncated data) models. Ignoring individual variability resulted in higher $L_{\infty,p}$ (respectively 3 and 5%, on average), lower K_p (18 and 14%) and, for the Richards model, lower M_p (19% on average) and smaller maximum growth increments (7% smaller) reached at smaller sizes (8% smaller) (Table 3).

5.3. Spatial variability of growth parameters

Growth parameters estimated for the Richards model varied geographically. The maximum growth rate (dL/dt_p^*) was estimated

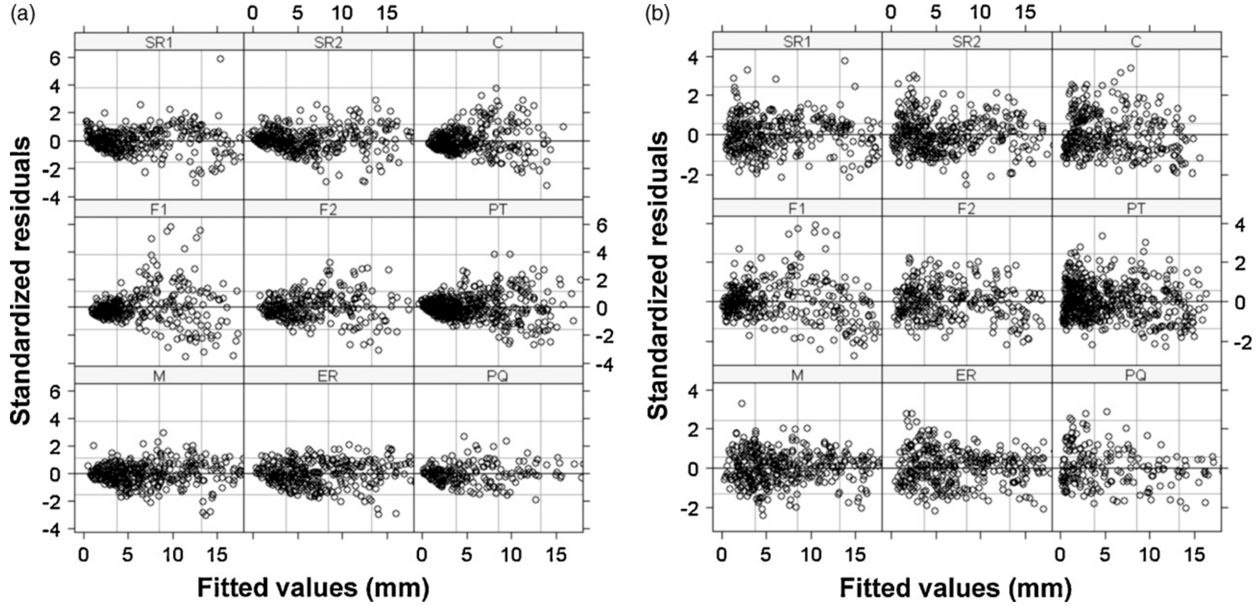

Fig. 8. Residuals of the von Bertalanffy models including variability among populations. (a) Variance assumed homogeneous. (b) Variance parameterized as a power function of the expected growth increment. Site labels as in Fig. 2.

Table 3
Parameters of the Richards and von Bertalanffy models estimated using mixed- and fixed-effects models. Fixed parameters differ among populations. dL/dt_p^* is maximum growth rate, and L_p^* the size at which growth rate is maximized.

a) Richards model, individual variability incorporated as random effects

Samples	$L_{\infty,p}$ (S.E.)	K_p (S.E.)	M_p (S.E.)	dL/dt_p^*	L_p^*
Punta Quiroga	69.77 (1.68)	0.44 (0.06)	0.71 (0.16)	13.25	21.41
Mendioroz	68.97 (1.30)	0.53 (0.05)	0.96 (0.14)	13.77	24.84
El Riacho	66.95 (1.30)	0.57 (0.05)	0.86 (0.14)	15.17	22.87
Punta Tehuelche	74.30 (1.29)	0.39 (0.05)	0.85 (0.14)	11.53	25.19
Fracaso 1	58.66 (1.25)	0.70 (0.05)	1.37 (0.15)	12.89	25.03
Fracaso 2	67.16 (1.39)	0.54 (0.05)	1.18 (0.16)	12.36	26.78
Conos	69.54 (1.51)	0.40 (0.059	0.91 (0.16)	10.72	24.45
San Roman 1	69.27 (0.91)	0.59 (0.03)	0.94 (0.10)	15.51	24.72
San Roman 2	62.76 (1.26)	0.56 (0.05)	0.83 (0.14)	14.07	20.93

Variance parameters	σ_{l_∞}	σ_k	σ_m	σ_ε	$\rho_{l_\infty k}$	$\rho_{l_\infty m}$	ρ_{km}
	4.69	0.16	0.48	2.34	−0.53	−0.38	0.89

b) Richards model, ignoring individual variability

Samples	$L_{\infty,p}$ (S.E.)	K_p (S.E.)	M_p (S.E.)	dL/dt_p^*	L_p^*
Punta Quiroga	70.61 (1.24)	0.36 (0.03)	0.58 (0.10)	12.14	13.71
Mendioroz	70.23 (0.84)	0.47 (0.03)	0.87 (0.08)	12.80	17.55
El Riacho	70.64 (1.03)	0.43 (0.03)	0.60 (0.08)	14.12	13.42
Punta Tehuelche	75.89 (0.82)	0.33 (0.02)	0.69 (0.08)	10.78	17.66
Fracaso 1	59.55 (0.62)	0.62 (0.04)	1.23 (0.10)	12.01	18.24
Fracaso 2	69.79 (1.05)	0.44 (0.03)	0.96 (0.11)	11.46	19.30
Conos	70.79 (1.23)	0.33 (0.03)	0.76 (0.10)	9.81	17.54
San Roman 1	72.55 (0.82)	0.45 (0.03)	0.69 (0.08)	14.21	15.20
San Roman 2	65.67 (0.86)	0.42 (0.03)	0.59 (0.08)	13.00	12.23

Variance parameters	σ_{l_∞}	σ_k	σ_m	σ_ε
	0	0	0	2.87

c) von Bertalanffy, individual variability incorporated as random effects

Samples	$L_{\infty,p}$ (S.E.)	K_p (S.E.)
Punta Quiroga	71.48 (0.88)	0.38 (0.01)
Mendioroz	64.85 (1.23)	0.37 (0.02)
El Riacho	68.35 (1.53)	0.36 (0.02)
Punta Tehuelche	73.34 (1.31)	0.31 (0.02)
Fracaso 1	69.36 (1.26)	0.39 (0.02)
Fracaso 2	75.84 (1.22)	0.27 (0.02)
Conos	60.19 (1.22)	0.42 (0.02)
San Roman 1	69.12 (1.35)	0.34 (0.02)
San Roman 2	71.08 (1.38)	0.25 (0.02)

Variance parameters	σ_{l_∞}	σ_k	σ_ε	$\rho_{l_\infty k}$	δ_ε
	5.33	0.05	0.54	−0.60	0.742

d) von Bertalanffy, ignoring individual variability

Samples	$L_{\infty,p}$ (S.E.)	K_p (S.E.)
Punta Quiroga	72.31 (1.29)	0.27 (0.01)
Mendioroz	74.17 (0.98)	0.20 (0.01)
El Riacho	73.18 (1.03)	0.32 (0.01)
Punta Tehuelche	78.67 (0.92)	0.29 (0.01)
Fracaso 1	63.73 (1.90)	0.33 (0.01)
Fracaso 2	74.02 (1.31)	0.27 (0.01)
Conos	75.56 (1.53)	0.20 (0.01)
San Roman 1	74.79 (0.87)	0.33 (0.01)
San Roman 2	66.98 (0.85)	0.33 (0.01)

Variance parameters	σ_{l_∞}	σ_k	σ_ε
	0	0	2.58

to be higher for populations from the West Domain (Table 3, Fig. 9a), consistently with the observed patterns in the data. A similar tendency was also captured by the von Bertalanffy model, but the differences were smaller (Table 3, Fig. 9b). The estimates of $L_{\infty,p}$ and K_p did not follow a clear geographic pattern in either the Richards or the von Bertalanffy models, nor did the estimates of L_p^* in the Richards model. Differences in the estimates of $L_{\infty,p}$, although statistically significant, were very small.

6. Discussion

6.1. Patterns

Growth of striped clams from San Jose Gulf, similarly to other marine invertebrates (Yamaguchi, 1975), is faster early during the post-larval life history, reaches a maximum at some intermediate age, and decreases in subsequent years. Within this general

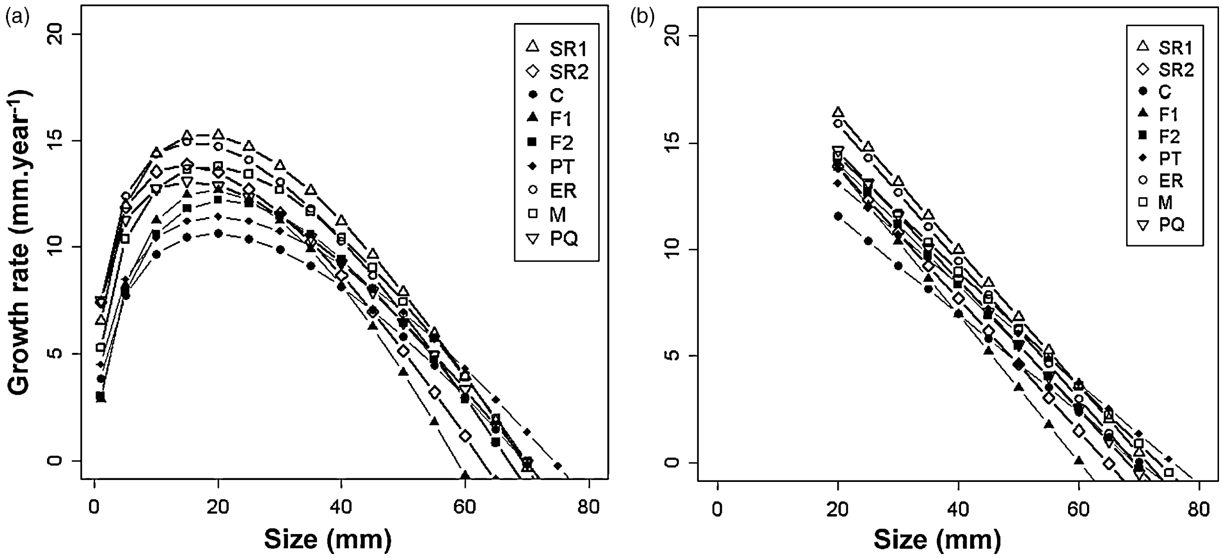

Fig. 9. Average growth rates predicted by the Richards (a) and von Bertalanffy (b) growth models for the different populations. The von Bertalanffy model was fitted to data truncated at the second growth ring. Filled symbols correspond to East Domain and open symbols to West Domain locations; site labels as in Fig. 2.

pattern there is substantial variation among populations and individuals. We found a clear geographical pattern, with two clusters of locations corresponding to domains separated by a thermal front running with a north–south direction. In the West Domain (i) growth rate of small clams (below size at inflection point) and maximum growth rate are highest and (ii) clams tend to experience maximum growth rate at a smaller size and a younger age (Fig. 5). Maximum size, on the other hand, did not show a clear geographic trend. Variation between domains is likely to be driven by environmental factors. Factors affecting the growth of suspension-feeding bivalves can operate at a hierarchy of spatial scales (Orensanz et al., 2005). At the mesoscale (domains, contrasts between locations) patterns may reflect the hydrographic regime or primary productivity in the overlaying water column, while at the microscale (within locations) variation could be related to clam density (e.g. Peterson, 1982), local gradients in sediment composition and seston flux (e.g. Grizzle and Morin, 1989), and modulation of water flow and deposition/resuspension by seafloor texture or biogenic structures (e.g. Peterson et al., 1984). Only mesoscale patterns may be explicable in our data; microscale variability (among individuals in each population) can be detected but not associated with specific factors. Much of the literature on mesoscale factors influencing bivalve growth in non-estuarine subtidal environments emphasizes the importance of near-bottom temperature (NBT), water flow, and sestonic food load, chlorophyll *a* concentration being a usual surrogate of the latter in the case of field studies.

Bioenergetic models predict that maximum size of poikilotherm marine invertebrates with indeterminate growth will be larger at relatively low temperature, and with higher food supply (Sebens, 1987, p. 396). In San Jose Gulf, during the growth season, concentration of chlorophyll *a* is higher in the West than in the East Domain (Ciocco, 1991; Esteves et al., 1986), while NBT is up to 2° lower in the West Domain (Amoroso, unpublished results). While the expectation would be for larger maximum size in the West Domain, there was no apparent difference between domains. Maximum size being equal, asymptotic growth models predict that growth rate increases with temperature (parameter *K* in the von Bertalanffy equation is theoretically and empirically correlated with temperature), and with food supply. Growth rate was consistently higher in the West Domain (most noticeably among young and/or small clams) in spite of NBT being comparatively low during the growth season, suggesting that the difference is related more to food availability than to temperature.

Food availability depends on sestonic load and flux. The latter is controlled by water flow, which can operate in different ways and at different scales. Experimental studies have shown that growth increases with water flow, at least below a certain threshold at which filtration is inhibited (Grizzle and Morin, 1989; Wildish and Kristmanson, 1979). The beneficial effect is generally associated with the flux of seston (Sebens, 1987). Mesoscale patterns observed in some coastal semi-closed systems are instead primarily associated with the relation between phytoplanktonic production and circulation. Production is often low near the inlet, either because inflowing water is cold and poor in nutrients (e.g. Long Island coastal lagoons, Weiss et al., 2007), or because tidal currents impede ageing of inflowing water rich in nutrients (e.g. Tomales Bay, Kimbro et al., 2009). In both cases maximum bivalve growth rate is reached at intermediate parts of the bay; productivity decreases towards the inner end of the bay either because water retention time is too long (Kimbro et al., 2009), or summer temperature is too high (Weiss et al., 2007). The San Jose Gulf bears some resemblance to low-inflow estuaries (LIE, Kimbro et al., 2009). Within the West Domain, relatively low growth rate at Punta Quiroga (lowest in the West Domain) is a presumable consequence of strong tidal currents, which do not allow the ageing of inflowing nutrient-rich water (Amoroso and Gagliardini, 2010). High growth rate was observed in locations where sheltering from direct eddy-driven flushing allows nutrient-reach water to mature and support relatively high primary production (Fig. 1b): El Riacho (214 gC m^{-2} year^{-1}; Ciocco, 1991) and San Roman (150–170 gC m^{-2} year^{-1}; Charpy and Charpy-Roubaud, 1980; Ciocco, 1991). Growth rate is low at Conos and Fracaso, at the head of the bay, where residence time is longest. High chlorophyll *a* concentration has been observed here in late winter (August), but remains low during the growth season. Punta Tehuelche, the pivotal "anchor" of the front at the south coast, is at the boundary between a high residence region to the east and intense eddies flushing to the west. Clam growth rate was low here, consistently with estimates of annual net primary productivity (89 gC m^{-2} year^{-1}; Ciocco, 1991).

Another suspension-feeding bivalve from San Jose Gulf, the Tehuelche scallop (*Aequipecten tehuelchus*), provides an interesting case in point. Previous studies (Amoroso, 2004; Ciocco, 1991;

Orensanz, 1986) found a recurrent pattern of clinal variation in individual growth rate, which coincides with the gradient described here for the striped clam: growth rate was highest near the entrance (San Roman) and lowest at Punta Tehuelche. This coincidence supports the explanation that differences in growth rate between populations of suspension-feeding bivalves from the West and East Domains of the San Jose gulf are due to higher productivity of the former.

6.2. Models

The life history of most marine bivalves involves a pelagic larva and post-settlement benthic juvenile to adult stages. Patterns of growth can be stage-specific (Urban, 2002): while growth of larval and post-larval stages (in linear dimensions) tends to be linear or exponential, adult growth is often asymptotic (Ebert, 1980; Ebert and Russel, 1993). For this latter reason, post-juvenile growth in marine bivalves is usually described with asymptotic functions, the von Bertalanffy model being the most popular. Because growth rate is assumed to decline linearly with size, at all sizes, the von Bertalanffy model may be unsuitable to represent growth over the complete life history (Clasing et al., 1994; Hart and Chute, 2009; Smith et al., 2001; Urban, 2002). A model with an inflection point, such as the Richards function (Ebert, 1980; Fletcher, 1975), might better describe post-settlement growth, including juvenile and adult stages (Clasing et al., 1994). In the case of the striped clam, however, the Richards model had structural limitations and failed to capture the sharp inflection point, which occurs around the second growth ring. In cases like this, when the data cannot be fitted with a single smooth function, multiple-stage growth models may be needed (see for example Laslett et al., 2002). In many fisheries applications, however, the interest is just to represent the growth of adult or post-recruit stages. If so, the use of simple asymptotic functions fitted only to the relevant portion of the data can prove a sensible option (Smith et al., 2001). In our case, using the von Bertalanffy model for individuals of age 2 and older avoided the statistical complications of multiple-stage models.

Contrast between domains in growth pattern was well captured by the Richards model (Fig. 9a), but not by the von Bertalanffy model (Fig. 9b). One reason may be that we truncated the data at a fixed growth ring (the second) corresponding to the average ring at which the inflection point occurred. This approach may have masked the spatial differences in the maximum growth rate by leaving out the maximum growth increments in populations in which growth rate peaked at an earlier growth ring.

Individual body growth is commonly described with average growth parameters, although in most length-at-age plots there is considerable variation around the average curve. Attention to individual variability is particularly important when modeling growth increment data, as ignoring it can result in substantial bias in estimated mean length-at-age (Sainsbury, 1980; Eveson et al., 2007). In striped clams all individuals have qualitatively similar growth patterns, but there is high variability in individual growth profiles. Accounting for this variability through random effects in all growth parameters affected the estimated average parameters: asymptotic sizes (L_∞) were smaller than estimated using fixed-effects models, while the estimates of the growth parameter (K), the curvature parameter (M), the maximum growth rate and the size at maximum growth rate were higher. As a result, growth increments at size predicted by the mixed-effects models were larger at intermediate sizes around the inflection point, and smaller on both extremes of the size range. These differences were also captured by the von Bertalanffy model. Similar results were reported by Hart and Chute (2009) who found that estimates of L_∞ and K based on a linear mixed-effects approximation of the von Bertalanffy model were respectively smaller and greater than those obtained without considering individual variability.

While longitudinal data provide information about underlying sources of growth variability, they bring the added complication of data correlation due to: (i) between-individual variability, as measurements on the same subject are more alike than measurements from different subjects, and/or (ii) within-individual variability, as measurements on a given subject are more alike the closer together they are in time (Hedeker and Gibbons, 2006; Zeger and Liang, 1986). Mixed-effects models accommodate the between-individual variability as random coefficients representing deviations from a population mean. The NLME library by Pinheiro et al. (2007) used in this analysis also allows for serial dependence of within-individual deviates modeled through different correlation structures. In the striped clam within-individual autocorrelation was not significant, a benefit of using growth increments instead of size-at-age data. A higher correlation can be expected in the latter case because departures from model predictions are – by definition – serially correlated if they result from random variation in the growth process (as opposed to measurement error). This is true even if the random variability of successive growth increments were independent. The use of growth increment data eliminates this source of autocorrelation and is also preferable when the analysis aims at separating spatial and temporal sources of variability in growth. It also eliminates the requirement to determine the absolute age of the individuals, which is often difficult when early rings are unclear (Hart and Chute, 2009).

6.3. Management implications

The existence of geographic differences in growth rate may be relevant for assessment and management, as fishing effort could differentially target areas of highest growth rate or productivity (Hart, 2001; Smith et al., 2001). Traditional models that use a dynamic pool assumption may misestimate the yield per recruit obtained from a fishery when spatial variation in fishing mortality is present (Hart, 2001). Fisheries that target sedentary stocks may benefit from the use of spatially specific management strategies, like the implementation of some type of area management and the setting of reference points that take into account geographic trends in productivity (Hart, 2001; Smith and Rago, 2004). In recent years some authors have proposed that management regulations for sedentary invertebrates could be fine-tuned to take into account growth variability at relatively fine spatial scales (Prince, 2005; Saunders et al., 2009). This may be a sensible proposition for species of abalone, which have high commercial value and self-seeded local populations. In the case of striped clams, observed variability may be too small to justify the use of management controls that vary spatially, as the complications involved in the enforcement of such rules may exceed potential gains. Simulation studies may be used to evaluate such trade-offs based on calculations of the anticipated benefits derived from the use of spatially explicit harvesting strategies.

Acknowledgements

The work described in this article is part of the thesis of Mrs. Escati-Peñaloza, and was conducted with support from a scholarship of the National Council for Scientific and Technical Research (CONICET), Argentina. We are most grateful to Ricardo Amoroso for satellite images and insightful discussions, and to Stephen Smith for a most thorough and helpful review. We acknowledge the collaboration of Ricardo Vera and Miguel Díaz, from Centro Nacional Patagónico (CENPAT, Puerto Madryn), as well as of José Ascorti and Pedro Oroquieta (artisanal fishermen), in the collection of the samples.

References

Amoroso, R.O., 2004. Heterogeneidad espacial en la dinámica de la metapoblación de vieira tehuelche (*Aequipecten tehuelchus*) del golfo San José. Universidad Nacional de la Patagonia (Puerto Madryn, Argentina), Licenciatura thesis, 55 pp.

Amoroso, R.O., Gagliardini, A., 2010. Inferring complex hidrographic processes using remote-sensed images: turbulent fluxes in the Patagonian Gulf and implications for scallop metapopulation dynamics. J. Coast. Res. 26, 320–332.

Cerrato, R.M., Keith, D.L., 1992. Age structure, growth and morphometric variations in the Atlantic surf clam, *Spisula solidissima*, from estuarine and inshore waters. Mar. Biol. 114, 581–593.

Charpy, L.J., Charpy-Roubaud, C.J., 1980. La production primarie des eaux du golfe San Jose (Peninsule Valdes, Argentine). III. Estimation de la production hytoplanctonique annuelle. Hydrobiologia 75, 225–229.

Ciocco, N.F., 1991. Differences in individual growth rate among scallop (*Chlamys tehuelcha* (D'Orb.)) populations from San José Gulf (Argentina). Fish. Res. 12, 31–42.

Clasing, E., Brey, T., Stead, R., Navarro, J., Asencio, G., 1994. Population dynamics of *Venus antiqua* (Bivalvia: Veneracea) in the bahía Yaldad, Isla de Chiloé, Southern Chile. J. Exp. Mar. Biol. Ecol. 177, 171–186.

Diggle, P.J., Heagerty, P., Liang, K.Y., Zeger, S.L., 2002. Analysis of Longitudinal Data, second ed. Oxford University Press, New York.

Ebert, T., 1980. Estimating parameters in a flexible growth equation, the Richards function. Can. J. Fish. Aquat. Sci. 37, 687–692.

Ebert, T.A., Russel, M.P., 1993. Growth and mortality of subtidal red urchins (*Strongylocentrotus franciscanus*) at San Nicolas Island, California, USA: problems with models. Mar. Biol. 117, 79–89.

Esteves, J.L., Solis, M., Cejas, J., Vera, R., 1986. Golfo San José: resultados de las campañas oceanográficas 1984/1985. Argentina: Report to the Chubut Province Administration (Argentina), 13 pp.

Eveson, J.P., Polacheck, T., Laslett, G.M., 2007. Consequences of assuming an incorrect error structure in von Bertalanffy growth models: a simulation study. Can. J. Fish. Aquat. Sci. 64, 602–617.

Fitzmaurice, G.M., Laird, N.M., Ware, J.H., 2004. Applied Longitudinal Analysis. John Wiley & Sons, Inc., Hoboken, NJ.

Fletcher, R.I., 1975. A general solution for the complete Richards function. Math. Biosci. 27, 349–360.

Grizzle, R.E., Morin, P.J., 1989. Effects of tidal currents, seston, and bottom sediments on growth of *Mercenaria mercenaria*: results of a field experiment. Mar. Biol. 102, 85–93.

Hart, D.R., 2001. Individual-based yield-per-recruit analysis, with an application to the Atlantic sea scallop *Placopecten magellanicus*. Can. J. Fish. Aquat. Sci. 58, 2351–2358.

Hart, D.R., Chute, A.S., 2009. Estimating von Bertalanffy growth parameters from growth increment data using a linear mixed-effects model, with an application to the sea scallop *Placopecten magellanicus*. ICES J. Mar. Sci. 66, 2165–2175.

Hedeker, D., Gibbons, R.D., 2006. Longitudinal Data Analysis. John Wiley & Sons, Inc., Hoboken, NJ.

Heino, M., Dieckmann, U., Godø, O.R., 2002. Measuring probabilistic reaction norms-for age and size at maturation. Evolution 56, 660–678.

Jerez, G., Ponce, F., Rivas, D., 1991. Análisis de la explotación del recurso almeja (*Venus antiqua antiqua* King y Broderip, 1835) en la Bahía de Ancud, Chile. Invest. Pesq. (Chile) 36, 3–16.

Kimbro, D.L., Largier, J., Grosholz, E.D., 2009. Coastal oceanographic processes influence the growth and size of a key estuarine species, the Olympia oyster. Limnol. Oceanogr. 54, 1425–1437.

Lasta, M.L., Ciocco, N.F., Bremec, C.S., Roux, A.M., 1998. Moluscos bivalvos y gasterópodos. El Mar Argentino y sus Recursos Pesqueros, vol. 2. Instituto Nacional de Investigación y Desarrollo Pesquero, Mar del Plata (Argentina), pp. 115–142.

Laslett, G.M., Eveson, J.P., Polacheck, T., 2002. A flexible maximum approache for fitting growth curvesto tag-recapture data. Can. J. Fish. Aquat. Sci. 59, 976–986.

Lindstrom, M.J., Bates, D.M., 1990. Nonlinear mixed-effects models for repeated measures data. Biometrics 46, 673–687.

Orensanz, J.M., 1986. Size, environment and density: the regulation of scallop stock and is management implications. Can. Spec. Publ. Fish. Aquat. Sci. 92, 195–227.

Orensanz, J.M., Parma, A.M., Turk, T., Valero, J., 2005. Population dynamics, assessment and management. In: Shumway, S. (Ed.), Scallops: Biology, Ecology and Aquaculture, second ed. Elsevier Publ., pp. 765–868.

Parma, A.M., Deriso, R.B., 1990. Dynamics of age and size composition in a population subject to size-selective mortality: effects of phenotypic variability in growth. Can. J. Fish. Aquat. Sci. 47, 274–289.

Peterson, C.H., 1982. The importance of predation and intra- and interspecific competition in the population biology of two infaunal suspension-feeding bivalves, *Protothaca staminea* and *Chione undatella*. Ecol. Monogr. 52, 437–475.

Peterson, C.H., Summerson, H.C., Duncan, P.B., 1984. The influence of seagrass cover on population structure and individual growth rate of a suspension feeding bivalve, *Mercenaria mercenaria*. J. Mar. Res. 42, 123–138.

Peterson, C.H., Beal, B.F., 1989. Bivalve growth and higher order interactions: importance of density, site and time. Ecology 70, 1390–1404.

Pilling, G.M., Kirkwood, G.P., Walker, S.G., 2002. An improved method for estimating individual growth variability in fish, and the correlation between the von Bertalanffy growth parameters. Can. J. Fish. Aquat. Sci. 59, 424–432.

Pinheiro, J.C., Bates, D.M., 2002. Mixed-effects Models in S and S-PLUS, second ed. Springer-Verlag, New York.

Pinheiro, J.C., Bates, D.M., DebRoy, S., Sarkar, D., The R Core Team, 2007. nlme: linear and nonlinear mixed-effects models. In: R Package Version 3.1-85.

Prince, J., 2005. Combating the tyranny of scale for haliotids: micro-management for microstocks. Bull. Mar. Sci. 76, 557–577.

Punt, A.E., Buckworth, R.C., Dichmont, C.M., Ye, J., 2009. Performance of methods for estimating size-transition matrices using tag-recapture data. Mar. Freshwater Res. 60, 168–182.

Quinn II, T.J., Deriso, R.B., 1999. Quantitative Fish Dynamics. Oxford University Press, New York.

R Development Core Team, 2007. R: A Language and Environment for Statistical Computing. R Foundation for Statistical Computing, Vienna (Austria).

Richardson, C.A., 2001. Molluscs as archives of environmental change. Oceanogr. Mar. Biol. 39, 103–164.

Richards, F.L., 1959. A flexible growth function for empirical use. J. Exp. Bot. 10, 290–300.

Sainsbury, K.J., 1980. Effect of individual variability on the von Bertalanffy growth equation. Can. J. Fish. Aquat. Sci. 37, 241–247.

Saunders, T.J., Mayfield, S., Hogg, A., 2009. Using a simple morphometric marker to identify spatial units for abalone fishery management. ICES J. Mar. Sci. 66, 305–314.

Schaalje, G.B., Shaw, J.L., Belk, M.C., 2002. Using nonlinear hierarchical models for analysing annulus-based size-at-age data. Can. J. Fish. Aquat. Sci. 59, 1524–1532.

Sebens, K.P., 1987. The ecology of indeterminate growth in animals. Ann. Rev. Ecol. Syst. 18, 371–407.

Smith, S.J., Kenchington, E.L., Lundy, M.J., Robert, G., Roddick, D., 2001. Spatially specific growth rates for sea scallops (*Placopecten magellanicus*). In: Kruse, G.H., Bez, N., Booth, A., Dorn, M., Hills, S., Lipcius, R., Pelletier, D., Roy, C., Smith, S.J., Witherell, D. (Eds.), Spatial Processes and Management of Marine Populations. University of Alaska Sea Grant, Fairbanks, pp. 211–231.

Smith, S.J., Rago, P., 2004. Biological reference points for sea scallops (*Placopecten magellanicus*): the benefits and costs of being nearly sessile. Can. J. Fish. Aquat. Sci. 61, 1338–1354.

Urban, J.H., 2002. Modeling growth of different developmental stages in bivalves. Mar. Ecol. Prog. Ser. 238, 109–114.

Verdinelli, M.A., Schuldt, M., 1976. Consideraciones preliminares sobre aspectos de la dinámica poblacional y reproductiva de la almeja rayada (*Ameghinomya antiqua*, King-Chionidae) en Punta Loma, golfo Nuevo-Chubut. Rev. Mus. La Plata (Argentina) (Zool.) 119, 183–202.

Wang, Y.-G., Thomas, M.R., 1995. Accounting for individual variability in the von Bertalanffy growth model. Can. J. Fish. Aquat. Sci. 52, 1368–1375.

Ware, J.H., 1985. Linear models for analysis of longitudinal studies. Am. Stat. 39, 95–101.

Weiss, M.B., Curran, P.B., Peterson, B.J., Gobler, C.J., 2007. The influence of plankton composition and water quality on hard clam (*Mercenaria mercenaria* L.) populations across Long Island's south shore lagoon estuaries (New York, USA). J. Exp. Mar. Biol. Ecol. 345, 12–25.

Wildish, D.J., Kristmanson, D.D., 1979. Tidal energy and sublittoral macrobenthic animals in estuaries. J. Fish. Res. Board Can. 36, 1197–1206.

Yamaguchi, M., 1975. Estimating growth parameters from growth rate data. Problems with marine sedentary invertebrates. Oecologia 20, 321–332.

Zeger, S.L., Liang, K.-Y., 1986. Longitudinal data analysis for discrete and continuous outcomes. Biometrics 42, 121–130.